

Pion-induced elastic and inelastic scattering above the 3,3 resonance

E. Oset

*Departamento Fisica Teorica and Instituto de Fisica Corpuscular,
Centro Mixto Universidad de Valencia Consejo Superior de Investigaciones Científicas,
E-46100 Burjassot (Valencia), Spain*

D. Strottman

*Theoretical Division, Los Alamos National Laboratory, Los Alamos, New Mexico 87545
(Received 19 February 1991)*

Results of Glauber model calculations of elastic and inelastic scattering from ^{12}C , ^{18}O , ^{40}Ca , and ^{48}Ca of pions having energy of 300 to 1200 MeV are presented. Experimental πN phase shifts including $l=0$ through 5 are used in the calculation. The f wave is important above 300 MeV and the g and h wave above 900 MeV. Effects of spin-flip are included. The model reasonably reproduces the 800 MeV/c data of Marlow although the inelastic scattering of the 2^+ of ^{12}C requires an enhancement of the quadrupole component consistent with the effective charge. The previously observed anomaly in ^{12}C in which a much larger oscillator parameter was required in pion scattering than in electron scattering disappears at higher energy. The $\sigma(\pi^-n)$ to $\sigma(\pi^+n)$ ratio is found to be appreciably different from expectations based on pion scattering from free nucleons.

I. INTRODUCTION

Recently, the study of pion-induced single- and double-charge exchange reactions^{1,2} in the energy regime of 300 to 550 MeV has begun at LAMPF. Results from elastic and inelastic-scattering reactions will become available shortly; these reactions will also soon be studied at even higher energies at KEK. And there already exists data³ from an experiment at 800 MeV/c with which we may compare calculations.

As one increases the pion energy and moves away from the dominating effect of the $\Delta_{3,3}$ resonance, other πN resonances are encountered. The $\sigma(\pi^-n)$ to $\sigma(\pi^+n)$ ratio for these new resonances will be much different from that of the $\Delta_{3,3}$; such resonances will provide an additional useful tool for investigating single-proton or -neutron excitations. Their study will shed additional light on the propagation of mesons in a nuclear medium. As one moves through the several resonances, the amount of spin flip will also change, thereby allowing a study of the role of the spin degrees of freedom.

In the region of the $\Delta_{3,3}$ resonance the ratio of $\sigma(\pi^-n)$ to $\sigma(\pi^+n)$ for free nucleons is 9:1. Among the initial results from pion-induced inelastic scattering from nuclei was the discovery that this does not necessarily apply to single-neutron transitions.⁴ Thus, in the inelastic excitation of the 2^+ of ^{18}O , the observed ratio was approximately two^{5,6} rather than the nine predicted from scattering on free nucleons. This phenomena found an explanation⁷ in the concept of the isoscalar effective charge already familiar from studies of $E2$ transitions. A pion may inelastically excite one of the many possible three-particle one-hole states. Since a proton may

equally well be excited from the core as a neutron, this has the effect of reducing the ratio from the pure neutron case. It was found the magnitude of the isoscalar effective charge needed in pion-induced reactions was of approximately the same magnitude as that required in electromagnetic transitions. More recently, an extensive work on ^{18}O comparing (e, e') and (π, π') has arrived at a similar conclusion.⁸

Whereas models of pion reactions in the region of the $\Delta_{3,3}$ resonance need include only s and p waves, calculations of pion-nucleus reactions in this higher-energy regime require the inclusion of several more πN partial waves. Parnell and Ernst⁹ have included d waves in their study of charge-exchange reactions and, hence, their model is thus valid only to around 400 MeV. In a recent theoretical study¹⁰ of pion-induced double-charge exchange it was found that the f wave becomes significant above 400 MeV, the g wave above 700 MeV, and the h wave above 1000 MeV. The effects of including the higher partial waves must also be checked in elastic and inelastic scattering; these transitions tend to be less sensitive to small details than is double-charge exchange and one may be able to use fewer partial waves.

Recent work on pion-induced elastic scattering has centered on an analysis of the 800-MeV/c data of Marlow *et al.*³ Both Mizoguchi and Toki¹¹ and Arima and Seki¹² employed a version of the Glauber model to calculate the elastic and inelastic scattering. In the former case the amplitudes were modified to fit the elastic data and were then applied to calculate the inelastic scattering. In our work we shall show the unmodified amplitudes give quite good results when compared with experiment.

In this paper we employ the Glauber model¹³ for which

the only input required is the free πN phase shifts and a shell-model description of the nuclear wave functions. It has the advantage of being microscopic yet has been found to provide reliable estimates of cross sections at resonance energies. With increasing pion energies, the model should be increasingly accurate as the πN cross section becomes increasingly forward peaked. At the pion energies with which we are dealing, the pion is less strongly absorbed than at the $\Delta_{3,3}$ resonance and details of nuclear structure can be important. Finally, the effects

of higher partial waves may be explicitly included.

In the next section we briefly review the formalism and details of our version of the Glauber model. In Sec. III we present results for elastic scattering and in Sec. IV results for inelastic scattering.

II. GLAUBER MODEL

The amplitude for (π, π') on a nucleus of A nucleons in the Glauber approach may be written as

$$F_{M_f M_i}(q) = \frac{ik}{2\pi} \int d^2b e^{i\mathbf{q}\cdot\mathbf{b}} \left\langle J_f T_f M_f \left| 1 - \prod_j^A (1 - \Gamma_j) \right| J_i T_i M_i \right\rangle, \quad (1)$$

where \mathbf{b} is the impact parameter, \mathbf{k} the incident pion momentum, $\mathbf{q} = \mathbf{k} - \mathbf{k}'$ is the momentum transfer, and Γ_j is the single-particle profile function

$$\Gamma_j(\mathbf{b} - \mathbf{s}_j) = \frac{1}{2\pi ik} \int d^2q h(q) e^{-i\mathbf{q}\cdot(\mathbf{b}-\mathbf{s}_j)} \quad (2)$$

in which \mathbf{s}_j is the projection of the vector position of a bound nucleon on the impact parameter plane. The variables \mathbf{k} and q in Eq. (1) are the laboratory variables while those in Eq. (2) refer to the πN c.m. system.

Equation (1) may be rewritten as

$$F_{M_f M_i}(q^2) = ik e^{i\Delta M \pi/2} \int_0^\infty b db J_{\Delta M}(qb) \Gamma_{M_f M_i}(b), \quad (3)$$

where

$$\Gamma_{M_f M_i}(b) e^{i\Delta M \phi_b} = \left\langle J_f T_f M_f \left| 1 - \prod_j^A (1 - \Gamma_j) \right| J_i T_i M_i \right\rangle.$$

In Eq. (3) $\Delta M = M_i - M_f$, ϕ_b is the azimuthal angle of \mathbf{b} , and $\Gamma_{M_f M_i}(b)$ is the nuclear profile function resulting from evaluating the nuclear matrix element. For zero-degree transitions, $q = 0$ and the Bessel function in Eq. (3) is one for $\Delta M = 0$ and zero otherwise. The integral then reduces simply to an integration of the profile function over impact parameter. One may thus ascertain the spatial origin of contributions to the angular distribution. The angular distribution is calculated by averaging over initial and summing over final states:

$$\frac{d\sigma}{d\Omega} = \frac{1}{2J_i + 1} \sum_{M_i, M_f} |F_{M_f M_i}(q^2)|^2. \quad (4)$$

The single-particle profile function of Eq. (2) is obtained from the πN amplitude:

$$h(q) = f^{(s)}(q) + \Theta \cdot \tau f^{(v)}(q) + i \left[g^{(s)}(q) + \Theta \cdot \tau g^{(v)}(q) \right] \sigma \cdot \hat{\mathbf{n}}. \quad (5)$$

In Eq. (5), the superscripts s and v refer to isoscalar and isovector amplitudes and the operators Θ and τ are isospin operators for the pion and nucleon, respectively. The πN amplitudes $h(q)$ are calculated using the usual partial-wave expansion rather than the commonly used exponential depending on q^2 .^{11,12,14} This avoids the approximation of choosing a parametric form for $h(q)$ and fitting its parameters to experimental data. The non-spin-flip amplitudes are obtained from

$$f = \sum_{l=0} [(l+1)f_{l+} + l f_{l-}] P_l(\cos \theta)$$

and the spin-flip amplitudes from

$$g = \sum_{l=1} [f_{l+} - f_{l-}] P'_l(\cos \theta) \sin \theta.$$

The πN phase shifts and inelasticity parameters used are those of Arndt's 1987 analysis.¹⁵ The πN amplitudes were calculated including partial waves up to an ℓ of 5. We have not included the effects of Coulomb scattering in this calculation. For ^{12}C and ^{18}O the effects are relatively small; for heavier nuclei it becomes more appreciable¹⁶ but as the energy increases Coulomb effects become less important.¹⁷

The initial and final nuclear wave functions were calculated as a sum of Slater determinants using a version of the Glasgow shell-model code.¹⁸ Because the wave functions are expressed in terms of Slater determinants, the many-body matrix elements of the Glauber operator, Eq. (1), may be expressed as the sum of $A \times A$ determinants. However, there is a complication that arises were charge exchange ($\pi^+ n \rightarrow \pi^0 p$) allowed to occur. Clearly, the intermediate π^0 cannot scatter off a nucleon until it has been created through an earlier charge exchange. Thus, there must be a time ordering implied. In the small-angle approximation, this is equivalent to

$$\prod_{j=1}^A \rightarrow \sum_{\text{perm}} (1 - \Gamma_1)(1 - \Gamma_2) \cdots (1 - \Gamma_A) \times \theta(z_2 - z_1) \cdots \theta(z_A - z_{A-1}). \quad (6)$$

One can easily demonstrate that if the Γ_j commute,

one need not worry about the time ordering and one can simply use Eq. (1). In general, one does not have

$$[\Gamma_i, \Gamma_j] = 0, \quad i \neq j$$

because the pion isospin operator Θ does not commute with itself. Since the isoscalar parts of the operator mutually commute, one could ignore time ordering if one were to retain only the isoscalar part.

It is known that the charge-exchange part of the πN amplitude is much smaller than the nonexchange term. The contribution of two charge exchanges leading back to the original charge were estimated to be small in Ref. 19 and a recent evaluation by Franco and Schlaile¹⁷ shows them to be negligible. We thus approximate the operator $\Theta \cdot \tau$ in Eq. (5) by $\Theta_z \tau_z$. This precludes the possibility of any charge-exchange processes but it allows the pion to interact differently with neutrons and protons or π^+ to be different from π^- scattering. There is then no difficulty with the time ordering.

With the inclusion of spin-flip, the evaluation of the $A \times A$ determinants then reduces to evaluating two smaller, block-diagonal determinants rather than four as in our previous work.¹⁹ Our method of evaluating the scattering amplitude has the virtue that the effects of antisymmetry, or Pauli correlations, are explicitly included. No free parameters (other than the oscillator parameter α^2) enter into the calculation.

The wave functions for mass twelve were obtained using the matrix elements of Cohen and Kurath.²⁰ For ^{18}O three model spaces were used to test the sensitivity of the inelastic scattering to the structure of the wave function. The model spaces included the $1d_{5/2}$, $1d_{5/2}$ and $2s_{1/2}$ orbits and, finally, the complete sd basis. In the former two cases, the two-body interaction used was that of Arima *et al.*²¹ which was determined by fitting levels in the $A=18-20$ mass region. Calculations in the complete basis used an interaction calculated by Kuo²² from the Reid nucleon-nucleon interaction.

Oscillator parameters obtained from electron scattering²³ are $\alpha^2 = 0.39 \text{ fm}^{-2}$ for ^{12}C and 0.319 fm^{-2} for ^{18}O . These values include corrections for the proton finite size. We have varied the oscillator parameter for ^{12}C to investigate whether the anomaly previously observed^{19,24-26} (a large α^2 required to fit the data) in the resonance region persists to higher energies. The oscillator parameters for ^{40}Ca and ^{48}Ca was simply obtained from the usual formula $\alpha^2 = 0.97A^{-1/3} \text{ fm}^{-2}$.

The matrix elements of the profile functions were evaluated as described in Refs. 19 and 27. Analytic expressions have been obtained for the single-particle profile function.²⁸ However, in the case of using an effective charge $\beta \neq 1$, the right-hand side of Eq. (2) is expanded, the quadrupole component is enhanced by a factor of β , and the integral is performed numerically.

III. RESULTS: ELASTIC SCATTERING

Results obtained with the Glauber model for elastic scattering of pions on a nucleus depend primarily upon

gross details of the nucleus such as the radius rather than on fine points of nuclear structure. Thus, elastic scattering can give some estimate of the accuracy of the Glauber model. In addition, it should determine, at least in principle, the oscillator parameter α^2 (which is the only undetermined parameter in our calculation) that should be used for inelastic scattering.

Historically, the first application of the Glauber model to the problem of medium-energy pions elastically scattering from nuclei was by Wilkin²⁴ and Schmit.²⁵ He assumed for the pion-nucleon amplitude $h(q)$ an exponential function depending on q^2 . The model was applied to ^{12}C for medium-energy pions and could successfully reproduce experiment only if a value for α^2 of 0.46 fm^{-2} was used which was much larger than the value suggested by electron scattering. A similar effect was obtained by Lee and Kurath²⁶ using an optical model although they preferred an even larger value, 0.51 fm^{-2} . In our earlier work¹⁹ on elastic scattering we also noted that data for 160 MeV pion scattering on ^{12}C was better reproduced if 0.51 fm^{-2} were used. Wilkin attributed this discrepancy in the value of α to deformation, while Lee and Kurath suggested it was due to higher orders of the density ρ in the optical potential. Although higher-order pieces of the optical potential are obviously missing in these approaches, the case of ^{12}C was particularly problematic, thus, the suggestions that at least part of the difficulty lay with nuclear-structure effects, most likely deformation.

As one moves away from the region of the $\Delta_{3,3}$ resonance, the nucleus becomes more transparent and higher powers of ρ should become less important. Indeed, the higher-order corrections in the region of the $\Delta_{3,3}$ resonance were mostly tied to Pauli blocking and absorption corrections.²⁹ However, as one increases the energy, the Pauli blocking effects become negligible and pion absorption, as shown in Ref. 27, also becomes progressively less important. However, the deformation remains although these effects may not be of the same magnitude as at lower energies. Indeed, we know that around resonance, because of the strong absorption, the reaction is rather peripheral, while at higher energies one will get a greater volume contribution. Hence, we might expect the effects of deformation to be more apparent near the resonance than at higher energies.

In Fig. 1 are shown our results for elastic scattering of 800 MeV/c incident pions compared with the data of Marlow *et al.*³ The calculation used a value of 0.39 fm^{-2} for α^2 , similar to the value given by electron scattering. The calculated angular distribution agrees remarkably well both in shape and magnitude with the data, particularly if one notes we have fixed all parameters *a priori* and not varied any in order to achieve a better agreement with experiment. The experimental results are slightly higher than theory for small angles and the theoretical minimum is deeper than experiment. However, no Coulomb effects that would mitigate the discrepancies have been included in this calculation. One

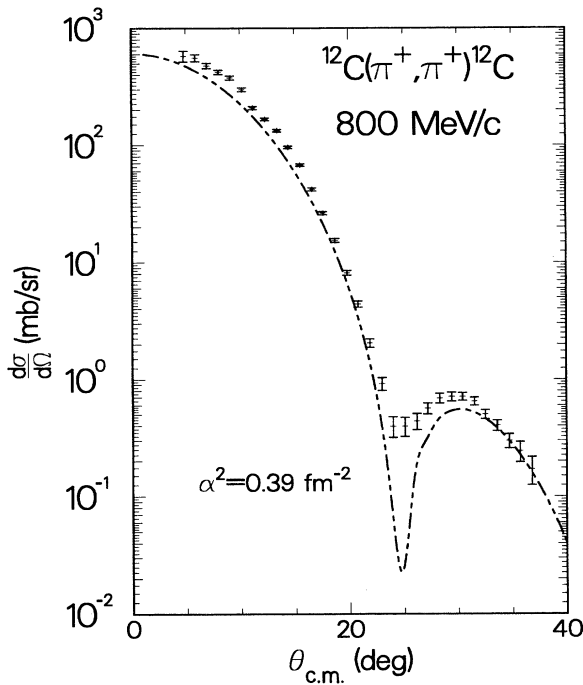


FIG. 1. Differential cross section in the center-of-mass system assuming partial waves through $l=5$ for $^{12}\text{C}(\pi^+, \pi^+)^{12}\text{C}$ scattering for 800 MeV/c pions; the experimental data are from Marlow *et al.*³ The contribution from spin-flip is included.

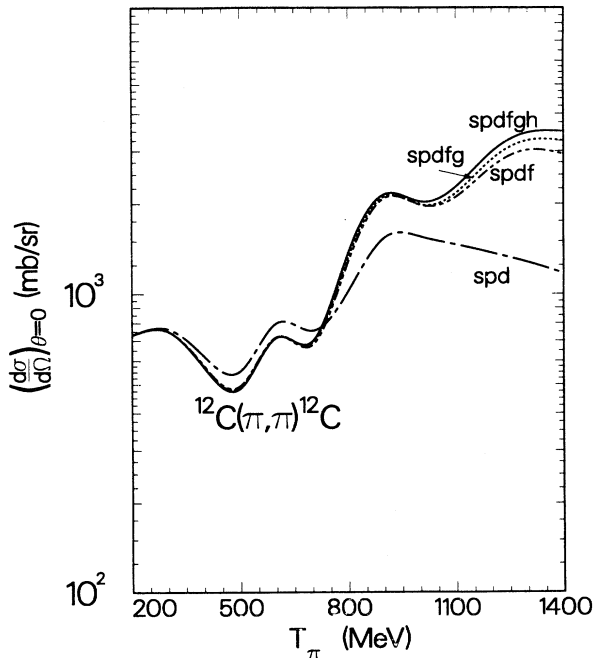


FIG. 2. Differential cross section at $\theta = 0^\circ$ in the laboratory system for the $^{12}\text{C}(\pi^+, \pi^+)^{12}\text{C}$ reaction as a function of the pion kinetic energy showing the contribution of the several partial waves. The solid line is the result including all partial waves up to $l = 5$. Effects of spin-flip are included.

may observe there appears to be no effect of the deformation at these energies. These results agree very well with those obtained in Ref. 11 before the πN amplitudes were varied to obtain a better fit with the data.

In Fig. 2 is shown the effect of adding additional partial waves in the πN amplitude on elastic scattering of pions from ^{12}C . The results include the contribution from spin-flip. The f wave becomes significant above 400 MeV. Unlike single-charge²⁷ and double-charge exchange,¹⁰ however, the g and h wave only begins to have an appreciable contribution above 900 MeV. We have also observed that these partial waves become important for inelastic scattering to the 2^+ state of ^{12}C at essentially the same energies as the charge-exchange reactions.

In Fig. 3 are shown the zero-degree cross sections for π^+ on ^{12}C , ^{18}O , ^{40}Ca , and ^{48}Ca as a function of the pion energy. The value of the cross section at zero degrees is appreciably affected by the Coulomb interaction which is not included in the calculation; thus the figure gives only the results due to the nuclear interaction and is a guide to the general systematic behavior with energy. The predicted energy dependence should remain unchanged after inclusion of Coulomb interaction. It is interesting that the cross section has minima around 500 and 700 MeV and local maxima near 600 and 850 MeV. These two peaks appear to reflect the two peaks that are clearly visible in the $\pi^- N$ cross section at these energies and which appear approximately at the energies of the $N^*(1440)$ and $N^*(1650)$ resonances. Unlike the case of pion-induced double-charge exchange,¹⁰ there is no indication of a reduction in the cross section near 1.2 GeV confirming that the deep minimum predicted in double-

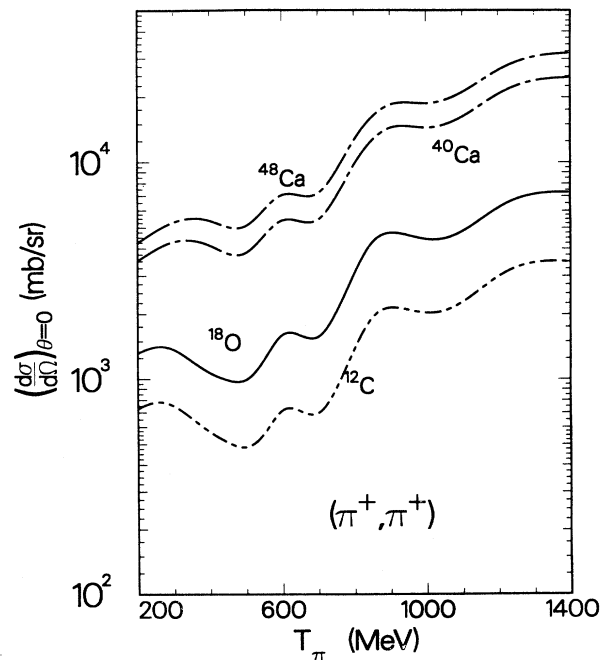


FIG. 3. Differential cross section at $\theta = 0^\circ$ in the laboratory system for the (π^+, π^+) scattering as a function of the pion kinetic energy for ^{12}C , ^{18}O , ^{40}Ca , and ^{48}Ca targets.

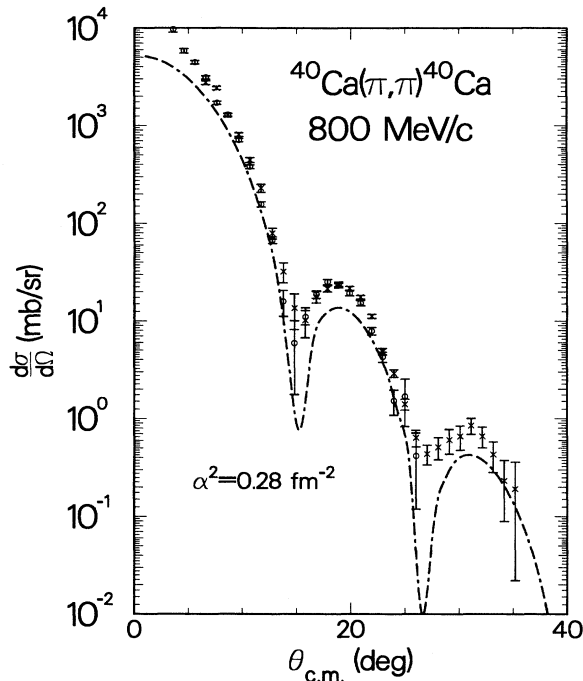


FIG. 4. Differential cross section in the center-of-mass system assuming partial waves through $\ell=5$ for $^{40}\text{Ca}(\pi^+, \pi^-)^{40}\text{Ca}$ scattering for 800 MeV/c pions. The contribution from spin-flip is included. The experimental results are from Marlow *et al.*³ The data for both π^+ (o) and π^- (x) are shown.

charge exchange is due to cancellation among the isovector amplitudes.

In Fig. 4 are shown angular distributions for π^+ scattering on ^{40}Ca at 800 MeV/c; the experimental results are from Marlow *et al.*³ The data for both π^+ and π^- are shown. The theoretical curves were obtained using the oscillator parameter $\alpha^2 = 0.28 \text{ fm}^{-2}$. The calculation reproduces the data remarkably well. The two minima are calculated to be at the same angle as experimentally observed. However, the theoretical results are systematically a bit low. Nevertheless, these results are quite remarkable if one recalls there are no free parameters to vary, free πN phase shifts were used, and no Coulomb interaction was included. Clearly, one could obtain results nearer to experiment were one to vary the parameters of the πN interaction. Using the Gaussian form for the πN interaction and the parameters suggested by Mizoguchi and Toki,¹¹ one does indeed find somewhat better agreement, particularly in the region of the second and third maxima and shallower minima occasioned by the use of a larger imaginary contribution to the interaction.

Figure 5 presents results of calculations of angular distributions for four energies that span the possible range of pion energies that could be obtained at KEK and PILAC. As expected from the presence of the Bessel function of order zero in Eq. (3), the angular distributions have the usual shape. The minima occur at decreasing angle as the pion energy increases. However, the actual magnitude of the cross section and the depth of the minima depend

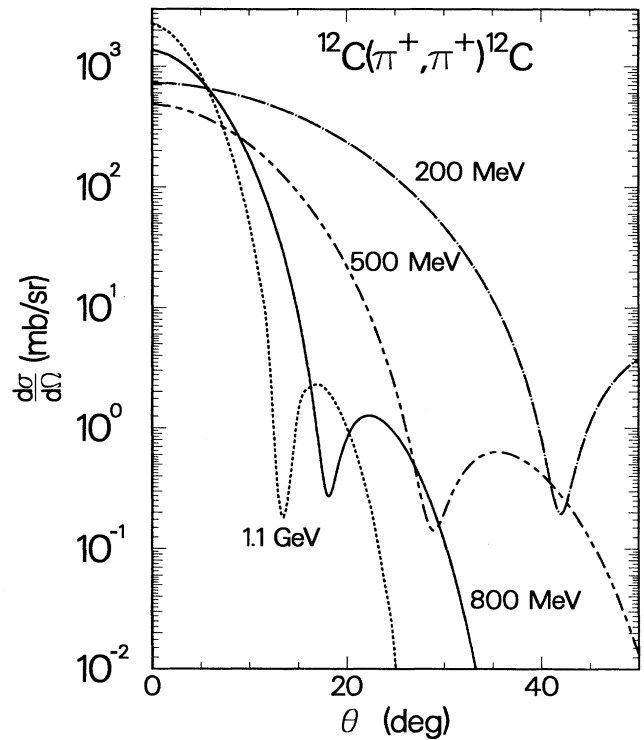


FIG. 5. Differential cross section in the laboratory system for (π, π) scattering on ^{12}C for four different pion kinetic energies. The oscillator parameter used was $\alpha^2=0.39 \text{ fm}^{-2}$. Effects of spin-flip are included. Partial waves up to $l = 5$ were included.

sensitively upon details of the nuclear profile function $\Gamma_{M_f M_i}(b)$. At all energies, $\text{Im}\Gamma_{M_f M_i}(b)$ has the shape of the nuclear density. The magnitude of $\text{Re}\Gamma_{M_f M_i}(b=0)$ decreases with increasing pion energy until around 600 MeV after which it varies only slightly with the bombarding energy. The $\text{Im}\Gamma_{M_f M_i}(b)$ is largest near 300 MeV at which energy it peaks near the nuclear surface. This reflects a substantial distortion at these energies which suppresses the contribution from small impact parameters. As the pion energy increases it becomes smaller until near 1 GeV $\text{Im}\Gamma_{M_f M_i}(b)$ is an order of magnitude smaller than $\text{Re}\Gamma_{M_f M_i}(b)$ and is roughly constant inside the nuclear surface.

The effect of including spin-flip on elastic scattering results is small. For pions incident on ^{18}O , at 300 MeV spin-flip affects the zero-degree results by less than one percent and in the region of the first minimum, it decreases the result by only two percent. At 1.2 GeV the effect of adding spin-flip is less than one percent for all angles less than 25° but begins to have a small effect in the region of the second minimum. The largest effect is around 600 MeV incident energy. Spin-flip decreases the forward angle scattering by approximately one percent and decreases the cross section in the region of the first minimum by 10%.

In summary, the results for ^{40}Ca and the ones described above for ^{12}C provide convincing evidence that

a zero-parameter Glauber model can give reliable estimates of elastic scattering for energies above the $\Delta_{3,3}$ resonance.

IV. RESULTS: INELASTIC SCATTERING

Unlike the case of elastic scattering, inelastic scattering is sensitive to details of nuclear structure. In particular, it is known^{7,8} that the magnitude (but not the shape) of the predicted cross section depends upon the size of the model space. In electromagnetic transitions the missing strength is taken into account through the mechanism of an effective charge. The physical picture is that the nucleon-nucleon interaction induces particle-hole excitations from the closed ^{16}O core and the gamma ray may be emitted from one of the many possible 3p-1h states. Similarly, a pion may inelastically excite such states. Since a proton may equally well be excited from the core as a neutron, this has the effect of reducing the ratio from the pure neutron case. Although we could include such excitations explicitly into the model space, the resulting basis would be too large to be manageable. Instead, we enhance⁷ the quadrupole component in each single-particle profile function by a factor of β just as one does with the effective charge in electromagnetic transitions. The salubrious effects are twofold: it increases the calculated cross sections to a value consistent with experiment and in the region of the resonance it reduces the $\sigma(\pi^-n)$ to $\sigma(\pi^+n)$ ratio. It was found⁷ that the magnitude of the isoscalar effective charge needed in pion-induced reactions was of approximately the same magnitude as that required in electromagnetic transitions.

In Fig. 6 are shown results for excitation of the 2^+ of ^{12}C by 800 MeV/c pions. The data are from Marlow *et al.*³ Only results for π^+ scattering are shown; because the Coulomb effects are small, the results for π^- differ by very little. Since the calculation does not include Coulomb and ^{12}C has isospin zero, the theoretical results for π^+ and π^- are identical.

Results of three calculations are given. The first employed no quadrupole enhancement and a value of α^2 (0.39) identical to that used for elastic scattering. This calculation seriously underestimates the data. The second calculation employed the same value of α^2 but used a quadrupole enhancement of 1.5. The resulting curve is much closer to the data although there is still disagreement for the most forward angles. Finally, the third calculation used a smaller value of α^2 (0.34) and an enhancement of 1.5. Although we have not attempted to fit the data, of the three this last curve most nearly follows the experimental points. The use of a smaller α^2 may simply be compensating for the tail of the harmonic oscillator wave functions; use of Woods-Saxon single-particle wave functions would have the same effect as using a smaller value of α^2 . However, there is still disagreement for the most forward angles. The shape of our calculated angular distribution is similar to that of the original calculations

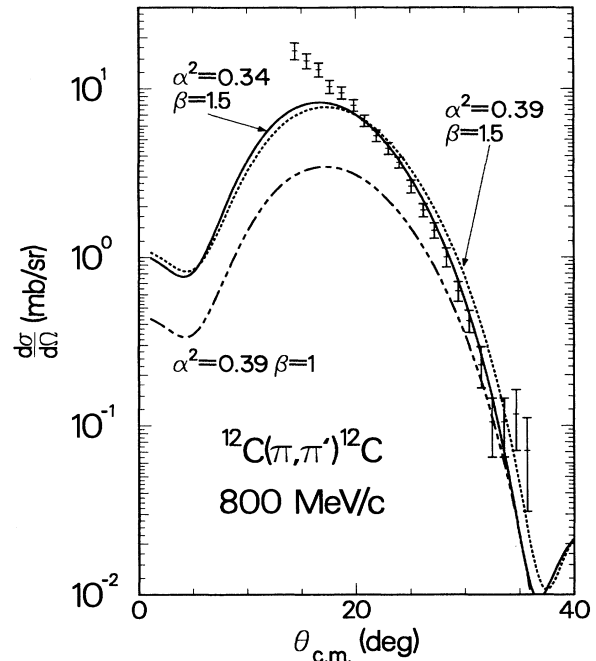


FIG. 6. Differential cross section in the center-of-mass system for (π, π') inelastic scattering to the 2^+ level of ^{12}C for 800 MeV/c pions; the experimental data are from Ref. 3. The theoretical curves are for $\alpha^2 = 0.39 \text{ fm}^{-2}$ (dash-dotted curve), $\beta = 1$, $\alpha^2 = 0.39 \text{ fm}^{-2}$, $\beta = 1.5$ (dotted curve) and $\alpha^2 = 0.34 \text{ fm}^{-2}$, $\beta = 1.5$ (solid curve). Partial waves up to $l = 5$ were included.

described by Marlow *et al.*³ who used the distorted-wave Born approximation to describe the reaction. Their results were slightly larger than are ours and thus were closer to the forward-angle data although still too low. Our results describe the intermediate-angle data somewhat better. We could essentially reproduce their curve were we to use a slightly larger value of the quadrupole enhancement.

In Fig. 7 are plotted angular distributions for four pion energies. The characteristic shape of these angular distributions — in which there is a shallow minimum at small angles followed by a maximum and then a much deeper minimum — arises from the two different contributions to the angular distribution. From Eq. (4) one sees that for a $J=0$ target the sum over the M_f components result in contributions from $\Delta M = 0, 1$, and 2. The $\Delta M = 1$ terms can arise only from spin-flip¹⁹ and for small angles, these are 2–3 orders of magnitude smaller than the contributions from $\Delta M = 0$ and 2; we shall not discuss them further. (This smallness arises in part from the fact the wave functions for ^{18}O are nearly pure $S = 0$. Transitions in nuclei for which the ground state has $S \neq 0$ could have appreciable contributions from spin-flip. These will be discussed elsewhere.) The relative weights of the $\Delta M = 0$ and 2 contributions depend upon the nuclear matrix element or profile function Γ .

Typically, the imaginary parts of the $\Delta J=2$ profile

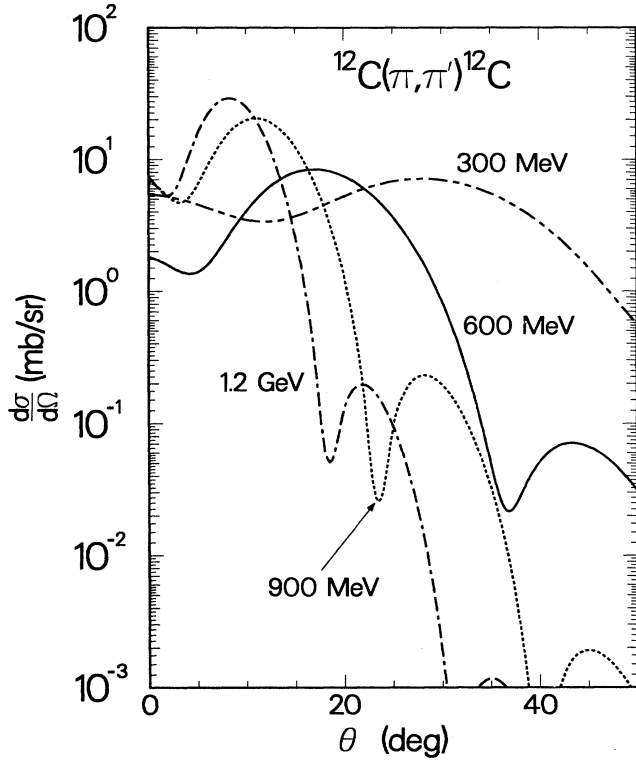


FIG. 7. Differential cross section in the laboratory system for the (π, π') excitation of the 2^+ level of ^{12}C for four different pion kinetic energies. An oscillator parameter $\alpha^2=0.39 \text{ fm}^{-2}$ and an enhancement of $\beta=1.5$ were used. Effects of spin-flip and partial waves up to $l=5$ were included.

function are much smaller than the real parts. $\text{Re}\Gamma_{\Delta M}(b)$ peaks near the nuclear surface, the $\Delta M=2$ profile function being a factor of 2 larger than the $\Delta M=0$ function. In addition $\text{Re}\Gamma_{\Delta M=0}(b)$ is negative near the origin and positive near the surface so that in the integration over b , there are significant cancellations that result in a small $\Delta M=0$ contribution to the small-angle cross section. When the quadrupole component is enhanced, the profile functions are merely scaled in magnitude.

In Fig. 8 are plotted the ratios of $\sigma(\pi^-n)$ to $\sigma(\pi^+n)$ for inelastic pion scattering to the lowest 2^+ and 4^+ of ^{18}O as a function of the pion kinetic energy. The angular distributions for π^- and for π^+ are nearly identical and the result plotted in Fig. 8 is the ratio at zero degrees. The curve labeled $\beta=1$ represents results assuming no additional effective charge and the curve labeled $\beta=1.5$ was obtained using a value for the quadrupole enhancement consistent with the results of both $E2$ transitions and pion inelastic scattering.

We only show one curve for the excitation of the 4^+ ; when the quadrupole component is enhanced with $\beta=1.5$, the ratio for the 4^+ changes by less than 20%. The use of the effective charge reduces the ratio at 300 MeV for the 2^+ from 13 to 4. At higher energies one obtains a similar result: using an effective charge always moves the

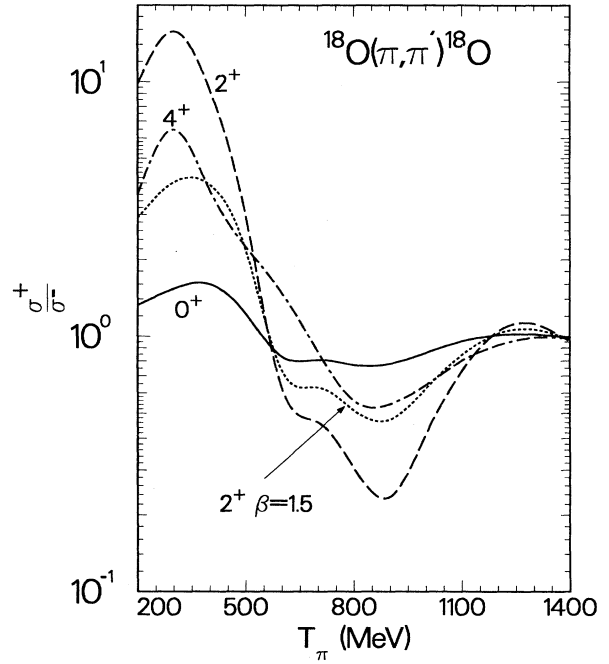


FIG. 8. Ratio of the forward-angle cross section for π^- to π^+ excitation of levels in ^{18}O as a function of bombarding energy. Effects of spin-orbit are included.

ratio nearer to unity — just as our physical picture would suggest. For both curves the ratio has a peak near 300 MeV after which it rapidly decreases. From 600 MeV until 1.2 GeV the 2^+ is seen stronger in π^+ scattering than in π^- , a reversal of the familiar situation around the resonance. Above 1.2 GeV the calculations suggest that the π^+ and the π^- should have similar cross sections. However, one should be aware that the πN phase shifts in this region are very poorly known. When more precise πN data for this energy region becomes available we anticipate the calculated results will change.

It is interesting to note that above $T_\pi=550$ MeV the ratio becomes smaller than one. The large values at the $\Delta_{3,3}$ peak simply show that the π^-n system is entirely in the $T = \frac{3}{2}$ channel whereas the π^+n is a mixture of $T = \frac{3}{2}$ and $T = \frac{1}{2}$. However, at the peaks seen in the elastic cross section around a pion kinetic energy of 600 MeV and 900 MeV — attributed to the N^* resonances — the ratios should be smaller than one since only the π^+ system has components in the $T = \frac{1}{2}$ channel. This is seen in Fig. 8 where one can observe some valleys, or relative minima, in this ratio at the place of the peaks of the elastic cross section.

In Fig. 9 we show the dependence of the results on the model space employed in the calculation. Each curve is the ratio as a function of energy of two calculations of the zero-degree cross section for π^+ excitation of the designated level in ^{18}O . The first calculation employed a model space restricted to only the $1d_{5/2}$ orbit while the second employed also the $2s_{1/2}$. As mentioned above the elastic cross section is unaffected by the choice of model

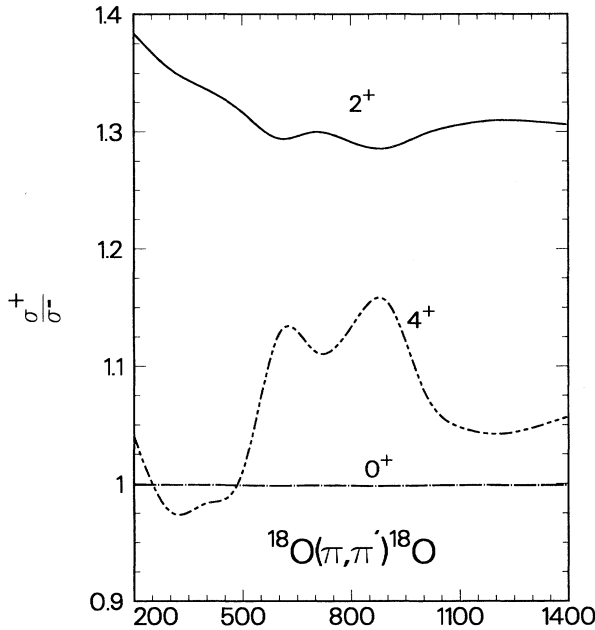


FIG. 9. Ratio for two choices of the model space of the forward-angle cross section for π^+ excitation of levels in ^{18}O as a function of bombarding energy. The curves show the results obtained with a $(1d_{5/2}2s_{1/2})$ model space divided by the results obtained with pure $(1d_{5/2})^2$ wave functions. Effects of spin-orbit are included.

space; this is consistent with the curve in Fig. 9 for the 0^+ . As already observed in double-charge exchange,³⁰ the inclusion of the $2s_{1/2}$ can greatly increase the cross section for certain transitions. In particular, the 2^+ transition is enhanced by 30 to 40% although the transition to the 4^+ is less affected. This latter result is because the 4^+ wave function is pure $(1d_{5/2})^2$ in our model; however, the $2s_{1/2}$ is part of the 0^+ ground state and as such can affect the transition to the 4^+ .

A reason the $2s_{1/2}$ is important is the absorption of the pion. The $2s_{1/2}$ single-particle wave function has a node and therefore more of its tail is outside the surface than for the $1d_{5/2}$. Thus, near 200 MeV where the absorption is the largest, the enhancement caused by inclusion of the $2s_{1/2}$ is at a maximum. The inclusion of the $1d_{3/2}$ in the model space has virtually no additional affect on these transitions.

V. CONCLUSION

In view of imminent experiments on pion-nucleus reactions above the delta resonance region, we have performed calculations of elastic and inelastic cross sections up to 1400 MeV pion kinetic energy. The tool used to study these reactions was Glauber theory, which requires the knowledge of only the elementary pion nucleon amplitude. We have used a partial-wave expansion including all partial waves up to $\ell=5$ where good convergence was found. We have used nuclear wave functions antisym-

metrized with respect to all the nucleons by expanding the wave functions in terms of Slater determinants using the Glasgow shell-model code.

The results for elastic scattering at 800 MeV/c — for which data are available — agree quite well with experiment. This suggests that previous disagreements found at energies around resonance should be attributed in part to the need of higher-order pieces of the pion-nucleus optical potential rather than to peculiarities of the nuclear wave function. On the other hand, we also noted that effects of intrinsic deformations that manifested themselves at resonance energies are not visible at higher energies because the scattering at these higher energies emphasizes the volume of the nucleus; this is in contrast to the resonance region where the strong absorption of the pion made the reaction very peripheral. The good results obtained here rely upon the elementary pion-nucleon amplitude and no need for a modification of this amplitude is observed. Our results imply that Glauber theory becomes more reliable as the energy increases. This is also supported from the fact that the higher energies make the eikonal approximation more reliable and on our previous findings that pion absorption, the most characteristic of the higher-order corrections, becomes negligibly small as the energy increases and Pauli blocking becomes equally negligible. All this indicates that the high-energy region offers a cleaner ground for investigation of nuclear-structure details than does the delta resonance region.

As a function of energy the elastic differential cross section at zero degrees grows nearly monotonically with energy, although showing some peaks that suggest N^* resonances are clearly visible in π^-p scattering. The inelastic-scattering cross section seems also to be well reproduced but it requires a renormalization of the quadrupole components to account for core polarization, in the same way as was needed to account for the electromagnetic $E2$ transitions.

The dominance of the region of $T_\pi = 600\text{--}1000$ MeV by the N^* resonances has an immediate repercussion on the ratio of π^- to π^+ inelastic scattering on nuclei with valence neutrons. This ratio is much bigger than unity around the delta region showing the $T = \frac{3}{2}$ character of the π^-n amplitude. In the N^* dominated region it is the π^+n amplitude, which has a $T = \frac{1}{2}$ component, that dominates, and we find values much smaller than 1 for the ratio. The values of this ratio for the excitation of the 2^+ component of a nucleus like ^{18}O are, however, appreciably changed when the quadrupole component is renormalized. The experimental investigation of this ratio as a function of the energy will undoubtedly provide interesting information on the mechanisms of core polarization.

Another finding of this work is that while the elastic cross section is rather insensitive to nuclear-structure details, inelastic scattering is rather sensitive and there is also an interesting energy dependence in the effects caused by modifications of the wave function.

One of the original goals of the pion factories which

produced a wealth of data around the delta resonance region was to investigate details on nuclear structure. Soon we learned that this task was not easy because the renormalization of the delta properties inside the nucleus was very important. With time we have learned much about this renormalization and about the interesting but complicated reaction mechanisms, but these complications in many cases blurred the possibility of obtaining clear and relevant information on nuclear structure. On the contrary, we are now in a region where the one-body mechanisms seem to dominate, and simple and intuitive pictures like Glauber theory can provide a good account of the reaction mechanisms. This region offers a cleaner ground to explore details of nuclear structure. On the other hand, by going to higher energies we move away

from the $T = \frac{3}{2}$ dominated region and enter a regime dominated by the $T = \frac{1}{2}$ resonances. This has drastic effects on the ratios of π^- to π^+ inelastic cross sections. The strong energy dependence of this ratio and other quantities still to be explored calls for a systematic experimental exploration of the whole energy range studied here.

ACKNOWLEDGMENTS

We wish to thank Ma Wei-Xing for his careful reading of the manuscript. This work was supported in part by CICYT, the Joint Spanish American Committee for Scientific and Technological Cooperation, and the U.S. Department of Energy.

-
- ¹S.H. Rokni *et al.*, Phys. Lett. B **202**, 35 (1988).
²A. L. Williams *et al.*, Phys. Lett. B **216**, 11 (1989).
³D. Marlow *et al.*, Phys. Rev. C **30**, 1662(1984).
⁴S. Iverson *et al.*, Phys. Rev. Lett. **40**, 17 (1978); Phys. Lett. **82B**, 51 (1979).
⁵S.J. Seestrom-Morris *et al.*, Phys. Rev. C **37**, 2057 (1988).
⁶C.L. Morris *et al.*, Phys. Rev. C **35**, 1388 (1987).
⁷E. Oset and D. Strottman, Phys. Lett. **84B**, 396 (1979).
⁸A. Hayes, P. J. Ellis, and D.J. Millener (unpublished).
⁹G.E. Parnell and D.J. Ernst, Phys. Lett. B **205**, 135(1988).
¹⁰E. Oset and D. Strottman (unpublished); Los Alamos National Laboratory Report No. LA-UR-90-3645.
¹¹M. Mizoguchi and H. Toki, Nucl. Phys. A **513**, 685 (1990).
¹²M. Arima and R. Seki, in *Proceedings of the LAMPF DCX Workshop, Los Alamos, NM, 1989*, edited by W. R. Gibbs and M. J. Leitch (World Scientific, Singapore, 1990); M. Arima, K. Masutani, and R. Seki (unpublished).
¹³R.J. Glauber, *Lectures in Theoretical Physics* (Interscience, New York, 1959), Vol. 1, pp. 315-414.
¹⁴R. H. Bassel and C. Wilkin, Phys. Rev. **174**, 1179 (1968).
¹⁵R. Arndt, computer code SAID, Phys. Rev. D **28**, 97 (1983).
¹⁶C. Garcia-Recio, E. Oset, L.L. Salcedo, M.J. Lopez, and D. Strottman, Nucl. Phys. (in press).
¹⁷V. Franco and H. G. Schlaile, Phys. Rev. C **41**, 1075 (1990).
¹⁸R. Whitehead, Nucl. Phys. A **182**, 615 (1972); R. R. Whitehead, A. Watt, B. J. Cole, and I. Morrison, in *Advances in Nuclear Physics* (Plenum, New York, 1978), Vol. 9.
¹⁹E. Oset and D. Strottman, Nucl. Phys. A **355**, 437 (1981); *ibid.* A **377**, 297 (1982).
²⁰S. Cohen and D. Kurath, Nucl. Phys. **73**, 1 (1965).
²¹A. Arima, S. Cohen, R.D. Lawson, and M.H. Macfarlane, Nucl. Phys. **108**, 94 (1968).
²²T.T.S. Kuo, private communication.
²³C.W. de Jager, H. de Vries, and C. de Vries, At. Data Nucl. Data Tables **14**, 479 (1974).
²⁴C. Wilkin, Nuovo Cim. Lett. **4**, 491 (1970).
²⁵C. Schmit, Nuovo Cim. Lett. **4**, 454 (1970).
²⁶T.S.H. Lee and D. Kurath, Phys. Rev. C **21**, 293 (1980).
²⁷E. Oset and D. Strottman, Phys. Rev. C **41**, 2356 (1990).
²⁸E. Oset and D. Strottman, At. Data Nucl. Data Tables **28**, 531 (1983).
²⁹E. Oset and L.L. Salcedo, Nucl. Phys. A **468**, 631 (1987).
³⁰E. Oset, D. Strottman, and G. E. Brown, Phys. Lett. **73B**, 393 (1978).